

# The Roving Wire-Breaking Technique: a low cost mobility measurement procedure for string musical instruments

Guilherme Orelli Paiva<sup>a,b,\*</sup>, Frédéric Ablitzer<sup>a</sup>, François Gautier<sup>a</sup>, José Maria Campos dos Santos<sup>b</sup>

<sup>a</sup> Université du Maine, ENSIM-LAUM, 1 Rue Aristote, 72000 Le Mans, France

<sup>b</sup> University of Campinas, UNICAMP-FEM-DMC, Rua Mendeleyev, 200, CEP 13083-970 Campinas, SP, Brazil

## ARTICLE INFO

### Keywords:

Musical acoustics  
Wire-breaking method  
Mobility measurement  
String musical instruments  
Modal analysis

## ABSTRACT

Bridge mobilities are usually used to characterize the couplings between the strings and the body of plucked or bowed string instruments. Such transfer functions are classically measured using impact hammer technique. An alternative method called wire-breaking method (also known as step relaxation method), introduced initially for the excitation of large structures is investigated in this paper. The method has been adapted to string instruments: it consists in placing a thin copper wire around the string in a position very close to the bridge saddle and pulling aside in the direction of interest until the wire breaks abruptly imparting a step function force to the driving point. When carried out with damped strings, the acceleration of the bridge measured with a miniature sensor provides a good estimation of transfer mobilities. The limits of the technique in terms of repeatability and signal-to-noise ratio are investigated making use of comparisons with results obtained by the classical impact hammer method. It is finally shown that the bridge admittances measured using the “Roving Wire-Breaking Technique” may be used to identify mode shapes components at the bridge using a high resolution modal analysis. Since no force sensor is needed to measure mobility, the technique is low cost and can be used in the instrument maker workshop for instrument modal characterization.

## 1. Introduction

The sound produced by string musical instruments is the result of interactions of several subsystems: the excitation mechanism, the strings, the instrument body, the air and the listener. In the acoustical guitars and violins, the most of the energy that will be converted into radiated sound is transferred to the body through the bridge. The energy flow from each string depends primarily on how strongly it is coupled to the body: the stronger the coupling, the quicker the energy is transferred to the body. The mobility (or mechanical admittance), which is a complex quantity defined as the ratio in the frequency domain between velocity and force, is an indicator of the string/body coupling. For plucked string instruments the mobility governs the compromise between duration and power. For bowed string instruments, the mobility is one of the key factors determining playability. When considering velocity and force in the directions perpendicular (out-of-plane) and parallel (in-plane) to the soundboard plane, the mobility takes the form of a 2-D matrix whose diagonal terms describe the degree of coupling with the body in each direction considered separately and whose cross terms describe the coupling between the two string polarizations.

Mobility measurements are typically made to characterize and compare string instruments [1–8]. Mobilities measured at the bridge of string instruments can be also used to feed several sound synthesis models for plucked [9,10] and bowed [11,12] string instruments based on the modal description of strings and body separately. In such hybrid methods, modal parameters of the body are obtained from experimental data while string modal parameters are defined from analytical models.

This work is directly linked to the development of a tool for instrument makers (PAFI, *Plateforme d'aide à la facture instrumentale*, available at <http://pafi.univ-lemans.fr/>) which aims at supporting the maker decisions when building or adjusting musical instruments. This tool consists of online post-processing packages, including hybrid sound synthesis, a low cost bridge mobility measurement system and a musical instrument database [1,2,6,13]. As a consequence, there is a need to develop a low cost methodology for measuring body modal parameters (frequencies, damping coefficients and mode shapes components at the coupling points).

The main goal of this paper is to investigate the capability of the wire breaking technique to play this role. Such technique is not widely used and consists in exciting the instrument body by placing a thin copper around a string very close to the bridge and pulling it until it

\* Corresponding author at: University of Campinas, UNICAMP-FEM-DMC, Rua Mendeleyev, 200, CEP 13083-970 Campinas, SP, Brazil.  
E-mail address: [pitupaiva@gmail.com](mailto:pitupaiva@gmail.com) (G.O. Paiva).

breaks. The limitations of this low cost technique in terms of signal-to-noise ratio and repeatability are pointed out. The paper is organized as follows: in the rest of the current section a bibliography review on the wire excitation technique is presented, followed by the statement of the problem of using the classical hammer method for measuring mobilities at the bridge of string instruments. Section 2 presents the principle of the wire-breaking method and the experimental setup used for the measurements presented in this paper. In Section 3, the limitations of the wire-breaking method are investigated by making comparisons with results obtained by the hammer method. A calibration method for mobility measurement is proposed in Section 4. Finally, in Section 5, the “Roving Wire-Breaking Technique” is used to identify mode shapes at the bridge from mobility measurements.

### 1.1. Bibliography review

The wire-breaking method is based on the analysis of the response of a structure to a step force. Also known in other fields as “step relaxation method”, this method has been investigated in the dynamic characterization of some engineering systems such as wind turbines [14,15], bridges [16–18] and launch vehicles [19], where mechanical excitations for modal testing are not so easy to produce (see Fig. 1). In the musical acoustics context, the use of a fine wire for imparting a transverse “pluck” was suggested in [20] and applied in [21]. Later, a copper wire was employed by Woodhouse [5] in two applications. Firstly, it was used for obtaining controlled pluck responses on classical guitars: the wire provides at the pluck position a repeatable excitation in terms of level of stress, in the direction of interest. The acoustic and vibration responses were recorded using a microphone and accelerometer, respectively, allowing comparisons with synthesized sounds. Secondly, the method was employed to measure mobility curves at the bridge of a classical guitar, which allowed to feed sound synthesis models. Calibrated mobilities were obtained by comparison with measurements obtained with impact hammer and vibrometer laser previously calibrated. In [22], a guitar sound synthesis has been obtained from a passive admittance modeling whose parameters were extracted from admittance curves measured at the bridge using the wire-breaking technique. In [23], mobility measurements on cellos using a copper wire were carried out with a pickup system mounted on the bridge to collect the input force signals at the string notches. The measurements were compared with hammer excitation and normal bowing: nothing fundamentally different was observed between those methods. The wire technique was also used in [24] for measuring the bridge impulse response on violins with completely damped strings: the string excited at the bowing position leads the breaking wire to impart an impulse that runs along the string and hits the bridge. In [25], the wire excitation allowed a controllable pluck at different positions: the recorded sounds using a microphone were submitted to a high resolution modal analysis and the modal contributions of string and body on different guitar sounds were identified. Finally, in [26], a copper wire has been

used to pluck a rigidly anchored string. Optical sensors were used to measure the resulting signals from which modal parameters were extracted via a high resolution method and used to feed the string damping model proposed in [27].

### 1.2. Statement of the problem

For a linear system, the mobility transfer function  $Y_{ij}(\omega)$  is defined in the frequency domain as the ratio between the velocity response  $V_i(\omega)$  at degree of freedom  $i$  due to the force  $F_j(\omega)$  applied at the degree of freedom  $j$ ,

$$Y_{ij}(\omega) = \frac{V_i(\omega)}{F_j(\omega)}, \quad (1)$$

where  $\omega$  is the angular frequency.

For bowed and plucked string instruments, the mobility measured at the bridge quantifies the conversion of string force into bridge velocity. Both string forces and bridge velocities are assumed to be composed by two orthogonal components, parallel and perpendicular to the soundboard, corresponding respectively to  $y$  and  $z$  directions as shown in Fig. 2, so that

$$\begin{bmatrix} V_y(\omega) \\ V_z(\omega) \end{bmatrix} = \mathbf{Y} \begin{bmatrix} F_y(\omega) \\ F_z(\omega) \end{bmatrix}, \quad (2)$$

where  $\mathbf{Y}$  is the  $2 \times 2$  mobility matrix defined as

$$\mathbf{Y} = \begin{bmatrix} Y_{yy}(\omega) & Y_{yz}(\omega) \\ Y_{zy}(\omega) & Y_{zz}(\omega) \end{bmatrix}. \quad (3)$$

The description above neglects both string and bridge longitudinal motions since the parallel and perpendicular components are much higher. It is also assumed that no torque is exerted on the body when forces are applied to the driving points, so that the component in the  $x$  direction is ignored (cf. [28]).

Mobility matrices measured at the string/bridge contact points of string instruments are usually used to feed models for sound synthesis [7,22,9]. The classical method used for measuring these transfer functions is based on the so-called hammer method: an impulse force is imparted at the point in the direction of interest by means of a miniature impact hammer and the resulting acceleration is measured by a laser vibrometer or a lightweight accelerometer mounted on the bridge. Fig. 2a depicts a typical experimental setup used for measuring mobilities at the bridge of classical guitars using hammer and accelerometer.

## 2. The wire-breaking method

Although the wire technique can be used for different types of excitation (see Section 1.1), this paper focuses on the use of this technique for mobility measurement at the bridge of string instruments. In the rest of this paper, therefore, wire-breaking method refers to the method that

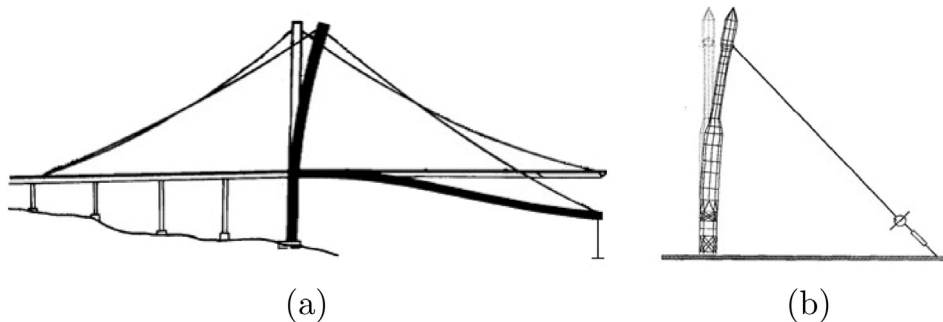


Fig. 1. Schematic illustrating applications of the step relaxation method to excite (a) a bridge [18] and (b) a launch vehicle [19].

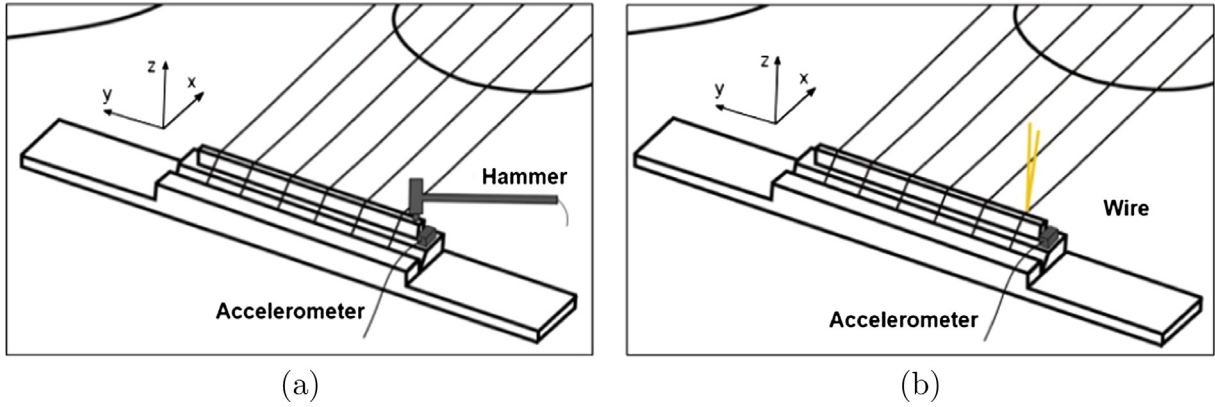


Fig. 2. Setups used for mobility measurements at the bridge of string instruments using (a) the hammer technique and (b) the wire technique.

uses a thin copper wire to excite the points where the strings make contact with the bridge. The wire is placed around the string in a position as close as possible to the saddle and then is pulled aside in the direction of interest until it breaks abruptly imparting a step function force to the excitation point. The measurement of the bridge response without the effect of string motion is feasible when the strings are completely damped. Under those conditions, the acceleration response to the wire excitation measured with a miniature sensor mounted on the bridge provides a good estimation of bridge mobilities without using any force sensor.

### 2.1. Equivalence between $v$ -impulse response and $a$ -step response

Let us consider a linear, time-invariant system. The mobility is defined as the ratio in the frequency domain of the Fourier transform of the velocity divided by the Fourier transform of the input force. In the hammer configuration, the impact force  $\mathbf{F}$  applied to the structure is written as  $\mathbf{F} = f(t)\mathbf{n}$ , where  $\mathbf{n}$  is the vector normal to the surface in the inward direction. In the breaking wire configuration, the step force is applied in the outward direction and is written as  $\mathbf{F} = u(t)\mathbf{n}$ , where

$$u(t) = \begin{cases} -f_0 & \text{if } t < 0 \\ 0 & \text{if } t \geq 0 \end{cases} \quad (4)$$

The Fourier transform of the velocity response due to the force  $u(t)$  is

$$V(\omega) = Y(\omega)U(\omega), \quad (5)$$

where  $U(\omega) = -f_0 \left( \pi \delta(\omega) - \frac{1}{j\omega} \right)$  is the Fourier transform of  $u(t)$ ,  $\delta(\omega)$  being the Dirac distribution. The acceleration response is therefore

$$A(\omega) = j\omega V(\omega) = -f_0 Y(\omega) j\omega \left( \pi \delta(\omega) - \frac{1}{j\omega} \right). \quad (6)$$

Eq. (6) shows that except for  $\omega = 0$ , the mobility of the system can be obtained from the Fourier transform of the acceleration response resulting from a step force excitation divided by the wire force:

$$Y(\omega) = \frac{A(\omega)}{f_0}. \quad (7)$$

### 2.2. Experimental setup

All the measurements reported in this paper were performed in the same laboratory environment. The results presented in Section 3 regard to measurements performed on a classical guitar. The instruments were placed in fixed positions using a guitar stand. The instruments were hung by the head and fixed on two of the stand feet using modeling clay so that the contact between the stand and the body only occurred at two

points. Before any measurement, the strings were tuned to their usual static tensions. All the measurements were carried out with damped strings.

For measurements using the hammer method, the force signal was provided by a miniature impact hammer PCB Piezotronics 086E80 whose head was mounted on a flexible beam clamped at its extremity. Such setup is a convenient way to control precisely the impact location and to avoid multiple hits. The impact was exerted on the saddle, as close as possible to the point where the E-string makes contact, as shown in Fig. 2a.

For measurements using the wire-breaking method, the step force excitation was provided by a thin copper wire with a diameter of 0.1 mm placed around the E-string in a position very close to the saddle (see Fig. 2b). For both hammer and wire-breaking methods, acceleration signals were collected by a lightweight accelerometer PCB Piezotronics 352C23 (mass 0.2 g) mounted on the bridge, close to the excitation point.

## 3. Results and discussion

### 3.1. Mobilities obtained with the hammer and wire-breaking methods

Typical mobilities measured at the bridge of a banjo, a Brazilian guitar, a classical guitar and a violin obtained by the hammer method are compared in Fig. 3, which highlights the difference of profiles of those four instruments. All the mobilities are characterized by numerous resonances, which induce variations around the averaged value over the useful frequency range. The mean mobility and the modal density are important features of the instrument soundboard [3]. Since the soundboard of the banjo is a membrane, its mobility is the highest up to 1500 Hz. On the other hand, the violin mobility is amplified in the vicinity of 2500 Hz, presenting the highest values: this feature is often referred to as the *bridge hill* [8,29,30]. The guitar soundboards (classical and Brazilian) have been shown to behave as plate-like systems: their mean mobilities and the modal densities are nearly independent on the frequency. This property is the one of a plate, whose equivalent parameters can be computed (cf. [31]).

Fig. 4 shows the mobility magnitudes and associated phases measured at the bridge of a classical guitar using the hammer method and the wire-breaking method taking into account the factor  $f_0$ , whose estimation is described in Section 4. For both magnitude and phase a good agreement can be observed up to 3000 Hz, which indicates that the experimental procedure used for estimating the wire-breaking force  $f_0$  provides a suitable calibration for the wire-breaking method. The agreement is less satisfactory at frequencies higher than 3000 Hz, where the hammer method leads to noisier results, revealing another advantage of using the wire-breaking method. With the wire-breaking

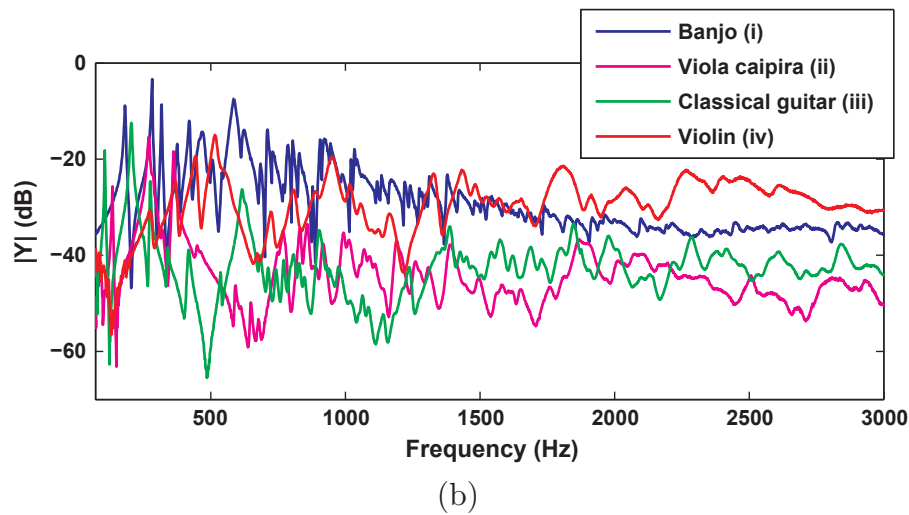
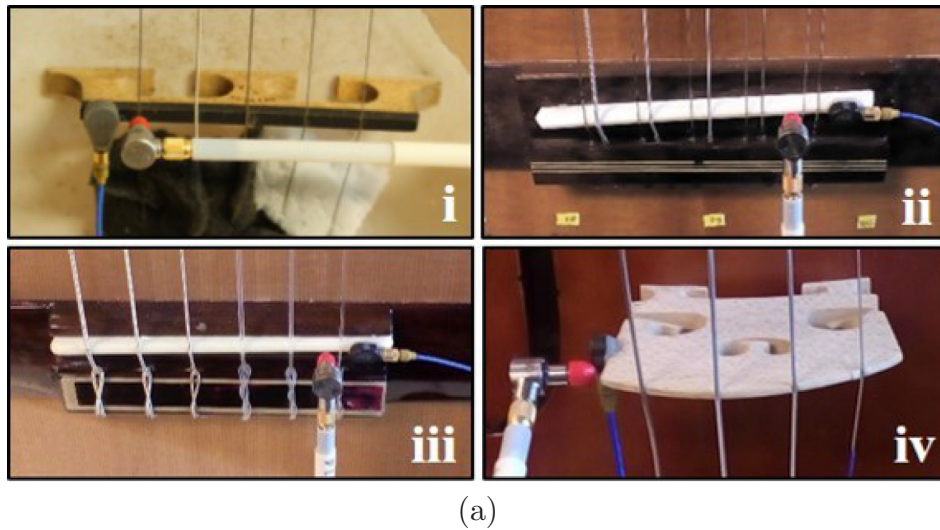


**Fig. 3.** (a) Experimental setups and (b) associated mobility magnitudes measured using the hammer method at the bridge of different instruments: (i) banjo (blue line), (ii) *viola caipira* (magenta line), (iii) classical guitar (green line), *viola caipira* (magenta line), and (iv) violin (red line). The dB scale reference is  $1 \text{ m s}^{-1} \text{ N}^{-1}$ . (For interpretation of the references to color in this figure legend, the reader is referred to the web version of this article.)

technique, the mobility is obtained using a Fourier transform of the measured acceleration. The signal used in practice starts at an instant defined by usual triggering conditions (i.e. when the acceleration signal exceeds a given threshold). When the signal is properly triggered, the phase of the mobility matches the one measured using the hammer technique, as shown in Fig. 4. Furthermore, the real part of the bridge mobility, which is a positive quantity regardless the frequency range, is proportional to the power injected into the structure. It can be checked that when the triggering conditions are properly defined in the wire breaking technique, this property can be used as a criterion for determining the appropriate triggering instant.

### 3.2. Repeatability of the wire-breaking method

In order to assess the repeatability of the wire-breaking method, five mobilities were measured under the same measurement conditions and compared in Fig. 5, which shows respective magnitudes and associated phases. It can be observed that, for both magnitude and phase, all the measurements lead to curves with substantially the same profile, which confirms the satisfactory repeatability of the method. Since the breaking force  $f_0$  is expected to be invariable for samples from the same reel and the choice of the excitation angles are controllable, the method

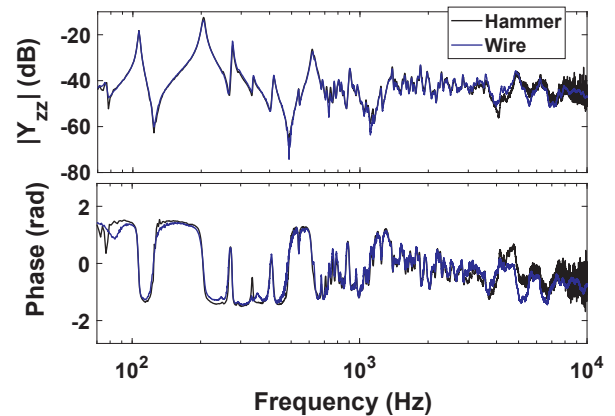


**Fig. 4.** Mobility magnitudes and associated phases measured at the bridge of a classical guitar using the hammer method (black lines) and wire-breaking method (blue lines) after calibration. The dB scale reference is  $1 \text{ m s}^{-1} \text{ N}^{-1}$ . (For interpretation of the references to color in this figure legend, the reader is referred to the web version of this article.)



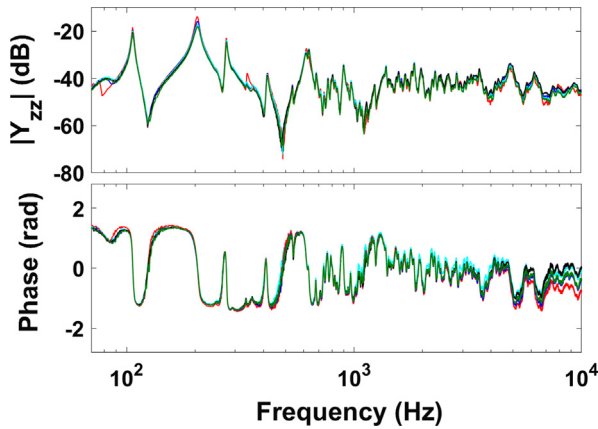


Fig. 5. Five mobility magnitudes and associated phases measured under the same conditions using the wire-breaking method. The dB scale reference is  $1 \text{ m s}^{-1} \text{ N}^{-1}$ .

allows reproducible measurements in different environments, by manipulation of different operators.

### 3.3. Influence of the wire diameter

The wire thickness is directly related to the magnitude of the wire breaking force  $f_0$  so that the choice of the wire diameter is determinant in the reliability of the measurements. Thicker wires may provide an excitation force  $f_0$  enough to move the instrument body while the wire is pulled aside, which leads to distorted measurements. Conversely, thinner wires may provide a low signal-to-noise ratio resulting in unreliable measurements. Fig. 6 shows a comparison between mobility curves measured using wires of three different diameters. Although measurements using the  $150 \mu\text{m}$  wire have shown to be the most satisfactory in terms of signal-to-noise ratio, the provided excitation force was too high so that the guitar moved from the support. On the other hand, as can be shown in the same figure, the  $56 \mu\text{m}$  wire provided the noisier results. The  $100 \mu\text{m}$  wire is, therefore, a good choice since it provides a good signal-to-noise ratio and a suitable force for the measured instrument.

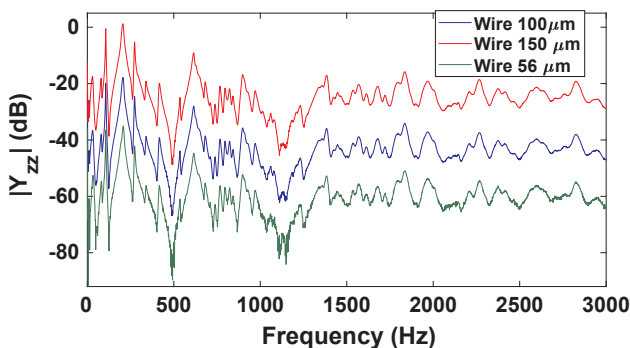


Fig. 6. Mobility magnitudes measured at the bridge of a classical guitar using wires of 3 different diameters:  $56 \mu\text{m}$  (green line),  $100 \mu\text{m}$  (blue line) and  $150 \mu\text{m}$  (red line). The green and blue curves are offset on the y-axis so that the comparison between the curves is feasible. The dB scale reference is  $1 \text{ m s}^{-1} \text{ N}^{-1}$ . (For interpretation of the references to color in this figure legend, the reader is referred to the web version of this article.)

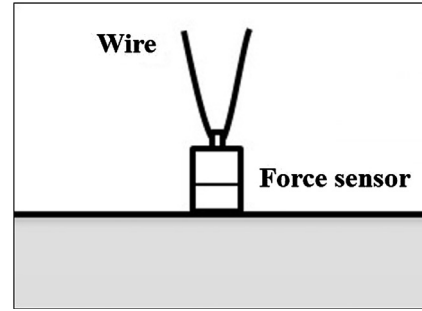


Fig. 7. Experimental setup used for measuring the wire-breaking force: the wire is attached to a fixed force sensor and pulled until it breaks.

## 4. Calibration of the wire-breaking method

Wire measurements require only one acceleration sensor for measuring mobilities on the bridge of the instruments. As a consequence, the breaking force  $f_0$  has to be determined in a preliminary phase in order to compute calibrated mobilities.

### 4.1. Measuring the wire-breaking force

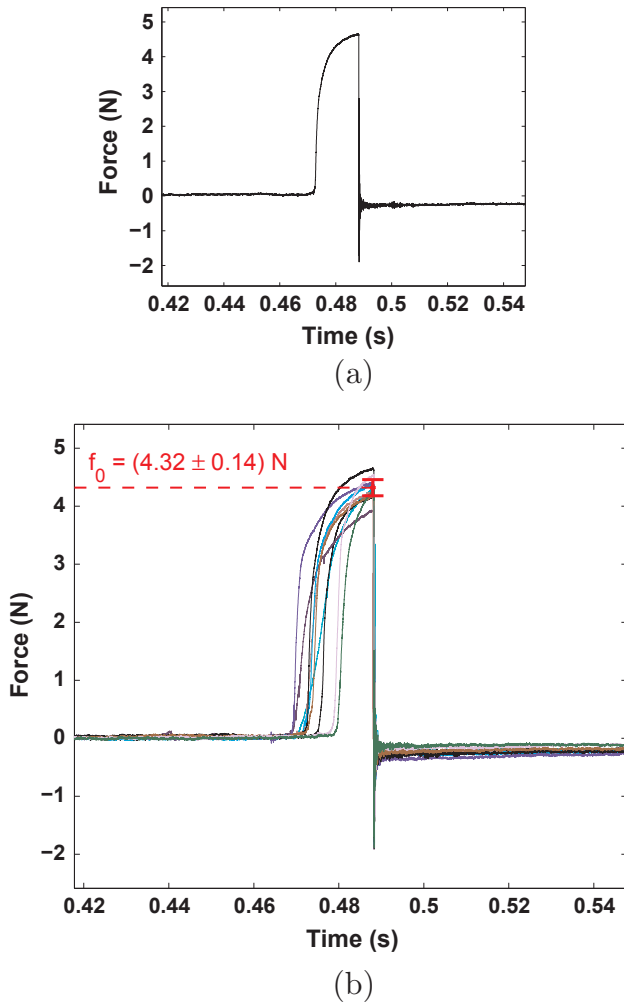
Fig. 7 shows the experimental setup used for measuring the wire-breaking force. The measurements consist in threading the wire through a rigid holder attached to the head of an impact hammer PCB Piezotronics 086C03, while the opposite hammer end is clamped onto a flat surface. In this way, the magnitude of the force measured by the hammer while the wire is pulled until it breaks is equivalent to the force exerted on the string. The value of  $f_0$ , therefore, is given by the maximum magnitude of the force curve measured in function of time, named the *wire-breaking force curve*.

Fig. 8a shows a typical wire-breaking force curve. For the sake of better visualization the signal of the measured force was inverted. At first, an upward force region is observed, which corresponds to the time interval that the wire is stretched. Then, the wire breaks and the measured force falls abruptly since no tension is exerted by the wire. Finally, the measured force features a damped oscillatory behavior that fades out progressively. Fig. 8b shows the comparison between 10 measures of the wire-breaking force curves obtained under the same conditions. Although all the curves have similar profiles, small differences can be observed, which can be due to slight variations of the gesture made by the operator while pulling the wire. Since the factor  $f_0$  is given by the maximum magnitude of the wire-breaking force curves, a value of  $f_0 = (4.32 \pm 0.14) \text{ N}$  is obtained as indicated in Fig. 8b. Noting that the wire-breaking setup consists of two strands that equally share the pulling load, the maximum force withstood by the strand that breaks is  $f_0/2$ , which corresponds to a stress of 275 MPa. This value is in line with typical ultimate tensile strength reported for enameled copper wire [31].

## 5. Application: roving wire-breaking technique

### 5.1. High resolution modal analysis

Since impact hammer measurements can be replaced by breaking wire measurements, can a modal analysis procedure be performed on these measurements with sufficient precision? To address this issue, a “Roving Wire-Breaking Technique” is defined and carried out on a Brazilian guitar, the *viola caipira*, which is composed of 5 pairs of strings (see Fig. 9). The aim is to determine the body modal parameters, i.e. frequencies, damping coefficients and mode shapes components at the 5 coupling points (denoted 1–5) in both directions (out-of-plane direction denoted  $z$  and in plane direction  $y$ ).



**Fig. 8.** (a) Typical measure (b) and ten measures of the breaking force curve of a 100  $\mu\text{m}$  wire. (For interpretation of the references to color in this figure legend, the reader is referred to the web version of this article.)

At the bridge of a string instrument, it is common that the accelerometer cannot be placed exactly on one of the coupling points. To circumvent this difficulty, a reference point denoted 0 is selected in such a way that a point mobility measurement at this point is possible. Responses resulting from the wire-breaking excitation are measured by a miniature accelerometer located at point 0. By moving the wire between the 6 measurement locations (5 coupling points + 1 reference

point) and by orienting the wire in both directions  $z$  and  $y$ , a set of 12 responses can be measured. Dividing by the calibration factor  $f_0$ , 12 impulse responses  $y_{ij}(t)$  can be obtained, where subscript  $i$  denotes the response degree of freedom (chosen here as  $i = 0z$ ) and subscript  $j$  denotes the excitation degree of freedom. For example  $y_{0z,1y}$  is the impulse response measured at point 0 in the direction  $z$  resulting from a wire break at point 1 and in the direction  $y$ . The modal analysis is performed in two steps.

- The first step concerns the identification of modal frequencies and damping coefficients using the high resolution technique ESPRIT described in [32,2]. This technique is based on the time-domain representation of the signal  $s(t)$  as a sum of complex exponentials, whose discrete representation  $s[n]$  is written as:

$$s[n] = \sum_{k=1}^{2K} a_k e^{-\alpha'_k n} e^{j(2\pi f'_k n + \varphi_k)} = \sum_{k=1}^{2K} b_k (z_k)^n, \quad (8)$$

where the  $K$  modes are characterized by their dimensionless modal frequencies  $f'_k$ , and their damping factors  $\alpha'_k$ , and are associated to amplitudes  $a_k$  and phases  $\varphi_k$ . The identification procedure consists in estimating the poles  $z_k = e^{-\alpha'_k + j2\pi f'_k}$  from which a collection of modal frequencies and modal damping coefficients can be obtained from

$$f_k = \frac{\arg(z_k)}{2\pi} F_s \quad \text{and} \quad \xi_k = \frac{-F_s \ln|z_k|}{2\pi f_k} \quad (9)$$

where  $F_s$  is the sampling frequency. The pole identification is performed using the ESPRIT algorithm, which is based on the decomposition of the input vector space onto two orthogonal subspaces, namely the signal and noise subspaces [33].

- The second step consists in estimating the modeling order and the mode shape components based on a fit in the frequency domain. For this purpose, the mobility  $Y_{ij}(\omega)$  is computed as the Fourier Transform of the response  $y_{ij}(t)$ . The modal model of  $Y_{ij}(\omega)$  is written as:

$$Y_{ij}(\omega) = \sum_{k=1}^K A_k H_k(\omega) \quad (10)$$

with

$$H_k(\omega) = \frac{j\omega}{\omega_k^2 - \omega^2 + j2\xi_k \omega_k \omega} \quad \text{and} \quad A_k = \Phi_{ik} \Phi_{jk}, \quad (11)$$

where  $\Phi_{jk}$  and  $\Phi_{ik}$  are the  $i$ th and  $j$ th components of the  $k$ th mode shape (mass normalized). The amplitudes  $A_k$  such that the modal sum of Eq. (10) best fits the measured mobility can be found by solving a least squares problem. Two aspects must be considered to

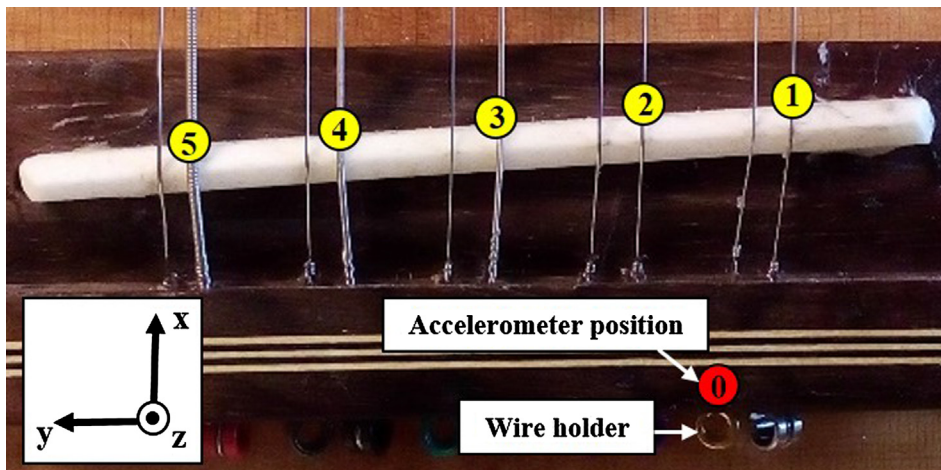


**Fig. 9.** Scheme used for estimation of mode shapes at the bridge of the *viola caipira* using the wire-breaking method. Point mobility is measured at point 0 (in red), where the accelerometer is fixed; the wire is. Points 1 to 5 (in yellow) are excited using the wire technique in the  $z$  and  $y$  directions. (For interpretation of the references to color in this figure legend, the reader is referred to the web version of this article.)

properly perform this least squares estimation. Firstly, it should be noted that the amplitudes  $A_k$  are real, whereas  $H_k(\omega)$  is complex-valued. Secondly, in the particular case of the point mobility  $Y_{0z,0z}(\omega)$ , the amplitudes  $A_k = \phi_{0z,k} \phi_{0z,k}$  are positive. To satisfy these two constraints, the estimation of amplitudes is first performed on the point mobility using a non-negative least squares (NNLS) procedure. The problem is expressed as

$$\min_{\mathbf{x}} \|\mathbf{C}\mathbf{x} - \mathbf{d}\|_2^2 \quad \text{with the constraint } x_k \geq 0 \quad \forall k, \quad (12)$$

where  $\mathbf{x} = [A_1 \dots A_k \dots A_K]^T$  is the vector of unknown modal amplitudes,

$$\mathbf{C} = \begin{bmatrix} \left| \begin{array}{c} \text{Re}(H_1(f_{\min})) \\ \vdots \\ \text{Re}(H_1(f_{\max})) \\ \text{Im}(H_1(f_{\min})) \\ \vdots \\ \text{Im}(H_1(f_{\max})) \end{array} \right| & \dots & \left| \begin{array}{c} \text{Re}(H_k(f_{\min})) \\ \vdots \\ \text{Re}(H_k(f_{\max})) \\ \text{Im}(H_k(f_{\min})) \\ \vdots \\ \text{Im}(H_k(f_{\max})) \end{array} \right| & \dots & \left| \begin{array}{c} \text{Re}(H_K(f_{\min})) \\ \vdots \\ \text{Re}(H_K(f_{\max})) \\ \text{Im}(H_K(f_{\min})) \\ \vdots \\ \text{Im}(H_K(f_{\max})) \end{array} \right| \end{bmatrix} \quad (13)$$

is a  $2N_{\text{freq}} \times K$  matrix whose columns form a basis of unitary modal responses and

$$\mathbf{d} = \begin{bmatrix} \text{Re}(H_{0z,0z}(f_{\min})) \\ \vdots \\ \text{Re}(H_{0z,0z}(f_{\max})) \\ \text{Im}(H_{0z,0z}(f_{\min})) \\ \vdots \\ \text{Im}(H_{0z,0z}(f_{\max})) \end{bmatrix} \quad (14)$$

is a  $2N_{\text{freq}} \times 1$  vector containing the measured mobility. The splitting of the unitary modal responses  $H_k(\omega)$  and the measured mobility  $H_{0z,0z}(\omega)$  into their real and imaginary parts is necessary to enforce that the estimated amplitude  $A_k$  are real. A characteristic of the NNLS procedure is that the solution  $\mathbf{x}$  consists of two subsets, one containing only strictly positive values and the other containing only zeros. Consequently, the procedure intrinsically provides a model order selection, since it does not use all poles identified by ESPRIT to fit the measured response. In the present application of the method, 47 modes were retained out of 165 candidate modes. Once the modal amplitudes of the point mobility have been estimated, those of the cross mobilities can be obtained by solving a standard least squares problem, which has the same form as Eq. (12) without the non-negative constraint. The identification of modal amplitudes for each cross-mobility measurement allows to determine the  $z$ - and  $y$ -components of mode shapes at the different coupling points  $A_k$  ( $j = 1z, 1y, 2z, 2y, \dots$ ).

Fig. 10a compares the point mobility  $H_{0z,0z}$  reconstructed from the NNLS solution to the measured mobility. A good fit is obtained in the frequency band of interest. The cross mobility  $H_{0z,0y}$  reconstructed from the standard least squares solution using the same modes is compared to the measured mobility in Fig. 10b. The signal-to-noise ratio of this measurement is lower due to the smaller amplitude of the soundboard vibrations in the  $y$ -direction. However, the reconstructed mobility overall well follows the measured mobility.

## 5.2. Synthesis of the mobility matrix

An example of reconstruction of the full mobility matrix at one coupling point is shown in Fig. 11. Note that a matrix concerns degrees of freedom whose physical access is difficult or impossible. Since the mobility matrix provide a full characterization of the instrument body

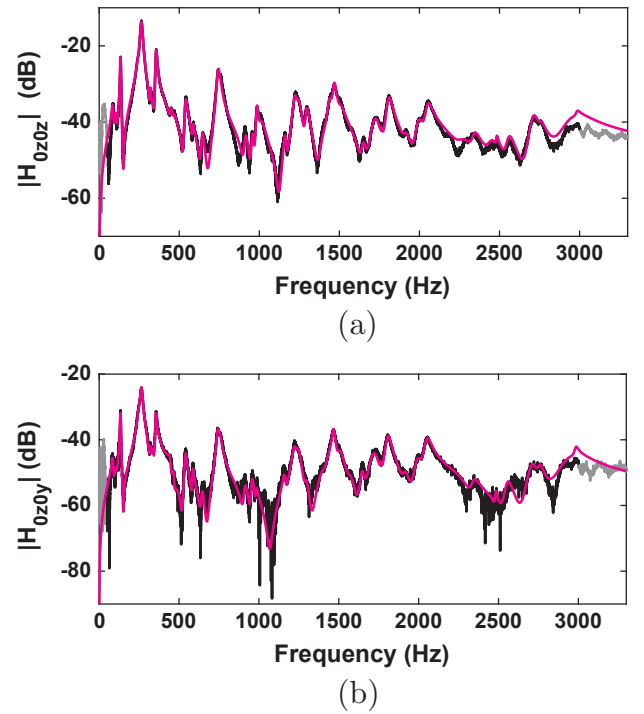
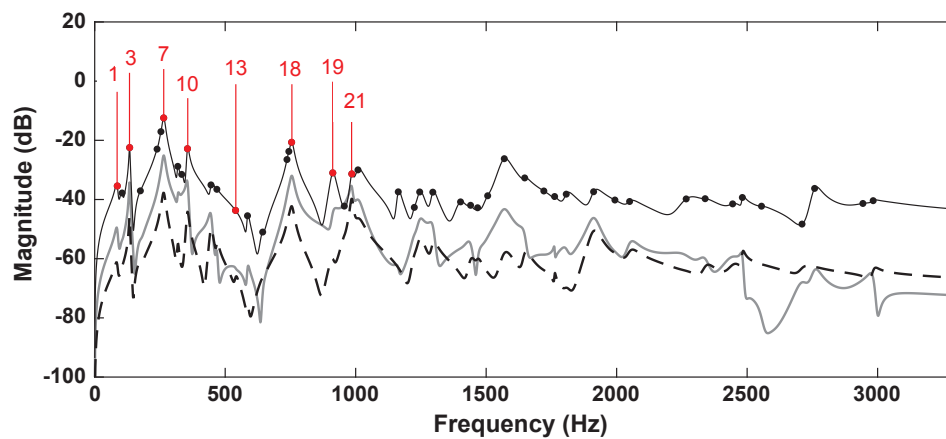


Fig. 10. Magnitude of (a) the direct mobility  $H_{0z,0z}$  and (b) the cross mobility  $H_{0z,0y}$  at the reference point 0. Black curve: measurement using the wire-breaking method. This curve is shaded below  $f_{\min} = 50$  Hz and above  $f_{\max} = 3000$  Hz to highlight the frequency range considered for modal amplitudes estimation. Magenta curve: reconstruction using 47 real modes obtained by the ESPRIT/NNLS procedure. (For interpretation of the references to color in this figure legend, the reader is referred to the web version of this article.)

at the coupling point, such a data is a useful input data for sound synthesis tools based on hybrid techniques.

## 5.3. Identification of mode shapes

Fig. 12a shows a selection of identified mode shapes at the bridge in the out-of-plane direction. Operating deflection shapes (ODS) of the instrument body at peak frequencies close to these modes are shown in Fig. 12b for comparison purpose. These ODS were obtained by exciting the bridge with an automatic impact hammer (Maul-Theet vImpact-60) and measuring the resulting velocity at numerous locations using a scanning laser vibrometer (Polytech PSV-500). The first mode shape identified by the procedure corresponds to a rigid-body mode of the instrument (see ODS a). Modes shape 3 and 7 are those of the A0 and T1 modes, which are the lowest modes significantly contributing to sound radiation of a guitar. They correspond to coupled motion of the top plate (see ODS b and c) and air piston in the soundhole through the stiffness of the air cavity. The resulting motion at the bridge involves in-phase, piston-like motion of the 10 coupling points. Mode 10 corresponds to the T2 mode, which is related to a top plate mode shape with a single longitudinal nodal line crossing bridge (see ODS d). As a result, it is the first mode where out-of-phase motion between coupling points occurs, namely between the treble and bass sides of the bridge. Although this may come as a surprise, piston-like motion of the bridge again occurs at some higher modal frequencies (e.g. modes 18 and 19). This can be understood when considering the related ODS (see ODS f and g), where the top plate exhibits more complex modal patterns but the bridge is not crossed by any nodal line. In contrast, mode 21 involves more rapid spatial variations of amplitude along the bridge, which is constrained to follow a motion of top plate involving more closely spaced longitudinal nodal lines (see ODS h). The knowledge of these relative amplitudes and phase relationships for the different



**Fig. 11.** Magnitude of the mobility matrix terms at coupling point 1 reconstructed using the modal parameters identified by the method. Direct out-of-plane mobility  $H_{1z1z}$  (black continuous line:), direct in-plane mobility  $H_{1y1y}$  (black dashed line) and cross mobility  $H_{1z1y}$  (gray continuous line). The dots on the out-of-plane mobility indicates the modes identified by the method and used for the mobility synthesis. The mode shapes of modes pointed out by their number are shown in Fig. 12a.

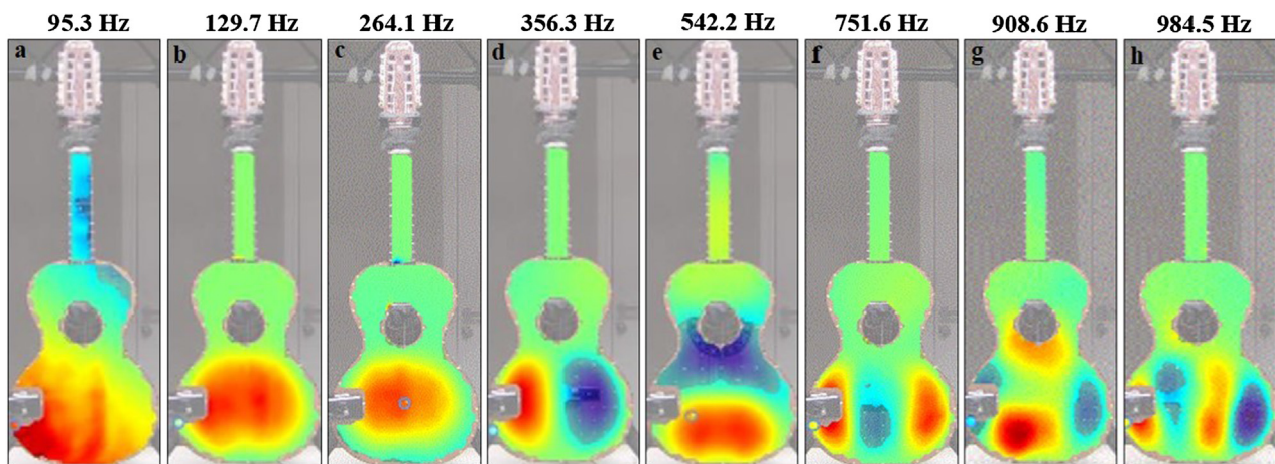
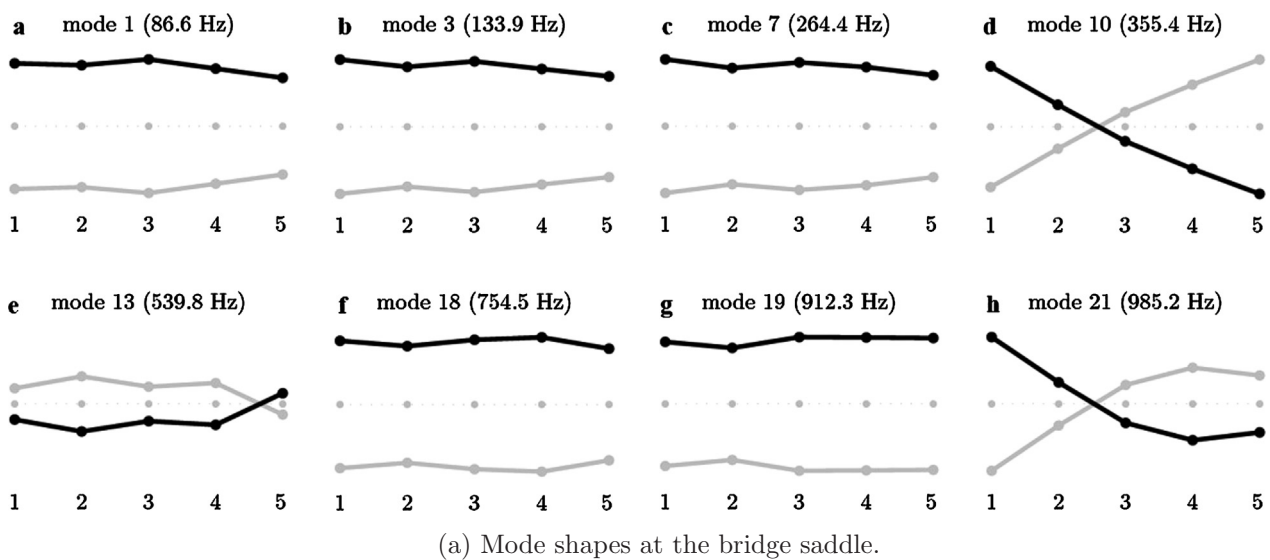


**Fig. 12.** (a) Examples of mode shapes at the bridge saddle and (b) corresponding operating deflection shapes of the *viola caipira* body.



modes can be useful in a model to account more accurately for sympathetic vibration between all strings.

## 6. Conclusion

This paper has investigated the capability of the wire-breaking method to accurately obtain the mobilities transfer functions at the bridge of a string instruments. Since no force sensor is required, this methodology is a low cost and well-adapted procedure for measurements in the environment of instrument maker workshop. The method was shown to be repeatable and provided results in reasonable agreement with the classical hammer method. A calibration method for mobilities obtained from wire-breaking measurement was proposed and validated. Finally, a modal analysis of the mobility curves measured at the bridge using the “Roving Wire-Breaking Technique” allowed the estimation of natural frequencies, damping factors and mode shapes at the string/bridge coupling points using a high resolution modal analysis. Such results can be used to feed sound synthesis models.

## Acknowledgements

The authors are thankful to the Brazilian Coordination for the Improvement of Higher Education Personnel Foundation (Grant 99999.010073/2014-00), National Council for Scientific and Technological Development in Brazil (Grant 141214/2013-9) and French National Center for Scientific Research for the financial support.

## References

- [1] Elie B, Gautier F, David B. Macro parameters describing the mechanical behavior of classical guitars. *J Acoust Soc Am* 2012;132(6):4013–24.
- [2] Elie B, Gautier F, David B. Acoustic signature of violins based on bridge transfer mobility measurements. *J Acoust Soc Am* 2014;136(3):1385–93.
- [3] Elie B. Vibroacoustic characterization of stringed musical instruments. application to the lutherie assistance, Ph.D. thesis. Ph.D. thesis, Université du Maine (France); 2012.
- [4] Woodhouse J, Langley R. Interpreting the input admittance of violins and guitars. *Acta Acustica United Acustica* 2012;98(4):611–28.
- [5] Woodhouse J. Plucked guitar transients: comparison of measurements and synthesis. *Acta Acustica United Acustica* 2004;90(5):945–65.
- [6] Elie B, Gautier F, David B. Estimation of mechanical properties of panels based on modal density and mean mobility measurements. *Mech Syst Sig Process* 2013;40(2):628–44.
- [7] Lambourg C, Chaigne A. Measurements and modeling of the admittance matrix at the bridge in guitars. In: *Proceedings of SMAC'93*; 1993, p. 448–53.
- [8] Bissinger G. Structural acoustics of good and bad violins. *J Acoust Soc Am* 2008;124(3):1764–73.
- [9] Woodhouse J. On the synthesis of guitar plucks. *Acta Acustica United Acustica* 2004;90(5):928–44.
- [10] Debut V, Antunes J, Marques M, Carvalho M. Physics-based modeling techniques of a twelve-string portuguese guitar: a non-linear time-domain computational approach for the multiple-strings/bridge/soundboard coupled dynamics. *Appl Acoust* 2016;108:3–18.
- [11] Inácio O, Antunes J, Wright M. Computational modelling of string-body interaction for the violin family and simulation of wolf notes. *J Sound Vib* 2008;310(1):260–86.
- [12] Demoucron M. On the control of virtual violins-physical modelling and control of bowed string instruments, Ph.D. thesis. Université Pierre et Marie Curie-Paris VI; Stockholm: Royal Institute of Technology; 2008.
- [13] Gautier F, Doutaut V, Fouilleul J. Lutherie tools: projet collaboratif entre ateliers de lutherie et laboratoires. *Musique Techn.* 2009;4:21–8.
- [14] Lauffer JP, Carne TG, Ashwill TD. Modal testing in the design evaluation of wind turbines. Sandia National Laboratories; 1988.
- [15] Osgood R. Dynamic characterization testing of wind turbines, Tech. rep. Golden (CO, US): National Renewable Energy Lab.; 2001.
- [16] Marecos J, Castanheta M, Trigo JT. Field observation of Tagus river suspension bridge. *J Struct Div* 1969;95(4):555–83.
- [17] Douglas BM. Quick release pullback testing and analytical seismic analysis of a six span composite girder bridge, Tech. rep.; 1976.
- [18] Ohlsson S. Modal testing of the tjorn bridge. In: *Proceedings of the 4th International Modal Analysis Conference*; 1986, p. 599–605.
- [19] Deiters TA, Hunt DL, Osborne E. A comparison of excitation methods to the taurus vehicle modal test. In: *Proceedings of the 12th international modal analysis*, vol. 2251; 1994, p. 26.
- [20] Reinecke W. Übertragungseigenschaften des streichinstrumentenstegs. *Catgut Acoust Soc Newsl* 1973;19:26–34.
- [21] McIntyre M, Woodhouse J. On the fundamentals of bowed-string dynamics. *Acta Acustica United Acustica* 1979;43(2):93–108.
- [22] Bank B, Karjalainen M. Passive admittance matrix modeling for guitar synthesis. In: *Proceedings of the conference on digital audio effects*; 2010, p. 3–8.
- [23] Zhang A, Woodhouse J. Reliability of the input admittance of bowed-string instruments measured by the hammer method. *J Acoust Soc Am* 2014;136(6):3371–81.
- [24] Turckheim F, Smit T, Mores R. Novel impulse response measurement method for stringed instruments. In: *Proceedings of the 20th international congress on acoustics*. Sydney; 2010, p. 2840–5.
- [25] Fréour V, Gautier F, David B, Curtit M. Extraction and analysis of body-induced partials of guitar tones. *J Acoust Soc Am* 2015;138(6):3930–40.
- [26] Paté A, Le Carrou J-L, Fabre B. Predicting the decay time of solid body electric guitar tones. *J Acoust Soc Am* 2014;135(5):3045–55.
- [27] Valette C, Cuesta C. *Mécanique de la corde vibrante*. Hermes; 1993.
- [28] Boutillon X. Model for piano hammers: experimental determination and digital simulation. *J Acoust Soc Am* 1988;83(2):746–54.
- [29] Durup F, Jansson EV. The quest of the violin bridge-hill. *Acta Acustica United Acustica* 2005;91(2):206–13.
- [30] Woodhouse J. On the bridge hill of the violin. *Acta Acustica United Acustica* 2005;91(1):155–65.
- [31] Hoekstra J. Properties and applications of enamelled wire. *Philips Tech Rev* 1938;3(2):40–7.
- [32] Ege K, Boutillon X, David B. High-resolution modal analysis. *J Sound Vib* 2009;325(4):852–69.
- [33] Badeau R, David B, Richard G. A new perturbation analysis for signal enumeration in rotational invariance techniques. *IEEE Trans Sig Process* 2006;54(2):450–8.